34th Annual International Conference of the IEEE EMBS
San Diego, California USA, 28 August - 1 September, 2012

Computational Methods for Objective Assessment of Conjunctival Vascularity

Reza Derakhshani, *Member, IEEE*, Sashi K. Saripalle, Plamen Doynov, *Member, IEEE*

***Abstract*— Assessment of vascularity of conjunctiva has many diagnostic and prognostic applications, thus creation of computational methods for its fast and objective assessment is of importance. Here we provide two different methods for estimation of conjunctiva's vascularity from color digital images, with our best results showing a correlation coefficient of 0.89 between the predicted and ground truth values using a committee of artificial neural networks.**

I. Introduction

Human eye is comprised of three layers: an external, fibrous tunic comprising the cornea and sclera; middle, vascular tunic comprising the iris, ciliary body, and choroid; an internal, nervous tunic, or retina. The sclera (white of the eye) is the posterior, opaque part of the external tunic and is covered by bulbar conjunctiva. The visible rich vascular network of the eye is confined to the stromal layer of the conjunctiva. Scleral stroma is supplied by the episcleral and, to a lesser degree, choroidal vascular networks. The choroidal vessels are responsible for the entire blood supply to the eye, which originate from the ophthalmic artery. The ophthalmic artery sprouts off the hyaloid artery, which passes through the embryonic choroidal artery, and the embryonic choroidal fissure. The ophthalmic artery gives off seven anterior ciliary arteries, which extend up to the front of the eyeball.

Various physiological factors may change the normal appearance of the conjunctival vasculature. External sources may engorge vessels causing conjunctival hyperemia and a reddish hue over the sclera. These external agents may include a variety of allergens and chemicals, foreign bodies, drugs and alcohol, trauma, infections, and dry eyes. Irritation of the eye may also result from infection or allergic conditions (conjunctivitis). In this case, the posterior conjunctival arteries become dilated and give a brick-red color to the conjunctiva. Inflammation of the cornea (keratitis) or of the iris and ciliary body (iridocyclitis) causes dilation of the anterior ciliary arteries resulting in a rose-pink band of "ciliary injection" [1].

Dumbelton et al. [2] discuss the response of vasculature to extended wear of hydrogel lenses of varying oxygen permeability (Dk). One of the immediate responses to the presence of contact lens in vascular region is limbal hyperemia. The authors conclude that mean limbal hyperemia remained constant for subjects who were wearing lens with high Dk compared to elevated mean limbal hyperemia for subjects who were wearing lens with low Dk.

Santodomingo-Rubido et al. [3] describe the effects of contact lens on conjunctival redness. They state that over time there is an increase in redness of conjunctiva in users of contact lenses. Also, there is an increase in papillary conjunctivitis for the first three months of lens wear, which stabilizes afterwards.

In one of the earliest studies in the field, Gardner [4] mentions the changes in appearances of conjunctiva across different subjects. His study involves subjects from difference ethnicities with ages ranging from 9 to 37 years. He observed that as age progresses the conjunctiva becomes less transparent. Interestingly, he states that a good diet would maintain opaque conjunctiva; as compared to a poor diet, which could lead to more conjunctival transparency.

Heath [5] describes the episcleritis as a benign, self-limiting condition of mild pain and an acute hyperemia, which could be either diffuse or nodular. Multiple recurrent episodes results in appearance of a translucent superficial sclera as a consequence of structure rearrangement of the sclera fibrils and physiochemical changes.

Thus, given the importance of conjunctival vasculature and its appearance, to quantify the effects of external as well as internal constraints on vasculature, two non-automated scales are defined: the Institute for Eye Research (IER) grading scale, previously known as Cornea and Contact Lens Research Unit scale CCLRU [6] and the Efron grading scale [7].

In a similar effort, Duenchet et al. [8] use a spectrophotometer to measure the conjunctival redness. They report that the redness in conjunctiva occurred in cyclic pattern, with least redness values observed in mid-day. Also, there was no significant cyclical pattern observed between eyes under observation.

Schulze et al. [9] describe image processing methods and compare them with traditional scaling methods [6, 7] to

* Research supported in part by a grant from Leonard Wood Institute.

Reza R Derakhshani, Ph.D., is an Associate Professor at the Department of Computer Science Electrical Engineering, University of Missouri at Kansas City, Kansas City, MO 64110-2499, (phone: (816) 235 5338; fax: (816) 235 5159; e-mail: reza@umkc.edu).

Sashi K. Saripalle is graduate student at the Department of Computer Science Electrical Engineering, University of Missouri at Kansas City, Kansas City, MO 64110-2499 (e-mail: ssqnf@mail.umkc.edu)

Plamen Doynov, is graduate student at the Department of Computer Science Electrical Engineering, University of Missouri at Kansas City, Kansas City, MO 64110-2499 (e-mail: plamendoynov@umkc.edu)

determine the redness of conjunctiva. They use fractals, which are scale invariant over a finite range of magnification, to quantify bulbar conjunctiva redness.

In summary, given the diagnostic and prognostic value of conjunctival vascularity and its effect on perceived scleral redness, it is important to develop automated, objective, and fast methods to evaluate the vascularity of bulbar conjunctiva. In this paper, we provide two image processing and machine learning based methods to evaluate the vascularity of conjunctiva using regular digital images. The methods generate a scalar measure of vascularity reflecting clear and dense visible conjunctival vasculature in a given RGB image. Of importance is the ability to measure the presence of actual vascular structures and their pronounced visibility, and not just scleral redness. Second, the described methods are data driven; the algorithms use adaptive learning for vascularity estimation from datasets scored by multiple human evaluators.

II. Methods and Procedure

A. Data

271 macro RGB eye images, captured by a consumer-grade digital camera while the subjects were looking to the left or right for maximum scleral exposure (Fig. 1), were used for this study (UMKC AHS IRB # 11-57e). Boxes were inscribed within scleral regions bounded by eyelids and the limbic boundary to include maximal conjunctival vasculature minus intruding periocular artifacts for the ensuing quantitative analysis. Next, five human observers were instructed to rate each image from 1 to 5, with 1 referring to the lowest perceived vascularity (i.e. no visually discernible conjunctival vasculature), and 5 pertaining to the highest level of vascularity (i.e. presence of dense, well defined, and highly visible vascular patterns). Thus, our ground truth is based on Human Visual System (HVS) assessment. No attempt was made to differentiate between physiological low vascularity and those caused by photographic aberrations such as defocus and overexposure, as the impact on the ensuing image processing routines are similar. In order to glean a more reliable ground truth from the HVS vascularity scores, we asked the observers to grade each conjunctival image over three separate occasions, resulting in 15 HVS vascularity scores for each image. Next, we discarded the images with high standard deviation (larger than 0.95, ten altogether) HVS scores as their vascularity estimates were deemed unreliable due to lack of HVS consensus. The 15 scores for each of the remaining 261 images were averaged to provide 261 scalar ground truth values for the forthcoming computational and image processing based vascularity estimation routines.

B. Methods and Results

To evaluate quality of the conjunctival vasculature we developed two different measures of vascularity, both yielding a scalar metric mimicking the corresponding HVS score for the given conjunctival RGB image. The first method is heuristic, and measures image vascularity as a linear combination of focus, morphological expansion of vascular structure, and color-differentiated patterns due to presence of vessels. The second, which is fully data-driven, measures conjunctival vascularity directly through evaluation of RGB layers of conjunctival images, and is based on a committee of neural networks. In each case, the methods were parameterized using the earlier mentioned set of 261 conjunctival images evaluated by multiple human observes (HVS), taken as the ground-truth for vascularity metric.

1. Heuristic Method

This method is basically a linear combination of three measures of image quality and vascularity. The first component is an Fourier-transform-based focus measure (FT), calculated as the ratio of high to low frequency energy contents of the image using its 2D-FFT, a well-known measure of image sharpness in digital photography in general and in ocular imaging in particular [10]. The incoming images are first enhanced by Contrasted-Limited Adaptive Histogram Equalization (CLAHE) of their green layer, another well-known method for enhancing conjunctival images [11]. The justification for inclusion of this no-reference focus quality metric is that, a conjunctival image populated with high contrast vasculature should provide a high FT due to the frequent and sharp transitions of its contents, whereas the lack of such patterns should reduce this effect.

The second component is based on the statistics of the differences between red, green, and blue layers of the conjunctival image. Given the red appearance of the conjunctival vasculature on top of the white sclera, they mostly absorb in blue and to a slightly lesser degree in green frequencies, whereas they are the least absorbent in red parts of the visible spectrum. Thus, vascular patterns, if apparent, are highly visible in blue and then green layers and not much in red (Fig 1). Thus, the fluctuations and visible patterns in the difference of red and green layers of the image should be higher than those of the difference between green and blue layers of the image. The second component of the heuristic method, Color Space (CS), is then defined as the ratio of the standard deviations of the aforesaid differential images calculated over pixel intensity values in R, G, and B matrices of the color image.

The third component, Morphological Vascularity (MV), is based on extent of vascular coverage after morphological transformations over the binarized conjunctival image. More specifically, first the green layer of the image is CLAHE-enhanced. Next, it is binarized using Otsu's method [12]. Next, the binarized image of the vasculature is further processed by the following morphological operations: closing, removal of spurs and isolated pixels, and then thinning of resulting binarized vasculature image to single pixel wide lines. Finally, MV is calculated as the percentage

of the scleral surface covered by the aforementioned processed vascular trees.

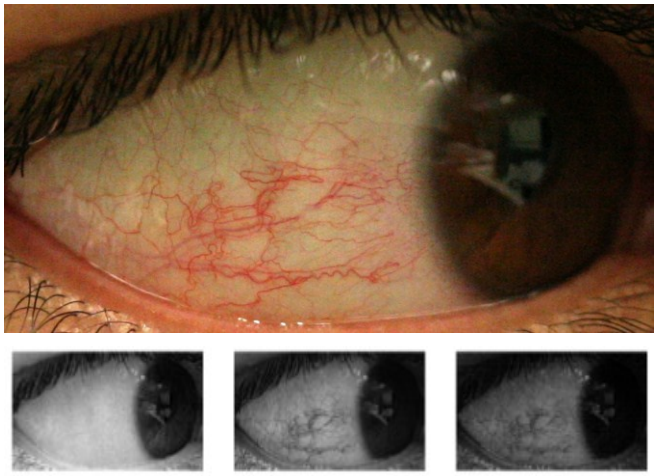

Figure 1. Top: an RGB color image of a human eye showing conjunctival vasculature on white of the eye. Bottom, from left to right: red, green, and blue layers of the image, showing prominence of conjunctival vasculature in green and blue layers of the RGB capture, as opposed to their weak presence in the red layer.

2. Heuristic Method Results

After running the aforementioned three metrics, it was observed that their correlation with HVS targets were not particularly strong. More specifically, the correlation coefficients of FT, CS, and MV vs. HVS were 0.3468, 0.4293, and 0.3900 respectively. Thus, using linear regression, we combined these three factors so that the linear combination better fits the HVS target, resulting in

$$\text{Vascularity} = \mathbf{a}*\text{FT} + b*\text{CS} + \mathbf{c}*\text{MV} \quad (1)$$

where, a is 0.0784821, b is 0.5798286 and c is 0.1855798.

The resulting new correlation coefficient between this multi-factor vascularity and HVS is 0.5853, larger than that of the participating components. Fig. 2 shows the lowest and highest vascularity images using this technique.

Figure 2. Conjunctival images with the lowest (left) and highest (right) vascularity as detected by the heuristic method.

3. Neural Network Methods

Artificial neural networks (ANN) have been known for their versatile and powerful system identification and classification capabilities. Given the right architecture and adequate and representative training data, neural nets can act as universal function approximators [13]. We may also use the properties of a multi-layered feed forward neural networks to avoid the onerous feature extraction and selection guesswork, and simply provide the RGB bitmaps directly to the ANNs and train the networks to match the input images with their corresponding HVS targets during supervised learning. Thus, here we used several ANNs with two hidden layers of various sizes (i.e. number of neurons in each layer), each with hyperbolic tangent activation functions, and a single node linear output layer. During the gradient descent training the first hidden layer is expected to find salient features out of the incoming images, and the second and third layers are expected to combine them into the desired output scores. To make sure of the validity of the results given nondeterministic convergence of ANNs to their solution during gradient descent, we randomly divided the data set into 70% training and 30% validation, and initialized and retrained each ANN configuration multiple times using validation based early stopping, and observed their average training and validation errors for choosing the best configuration (i.e. the number of nodes in the first and second hidden layers resulting in best training and validation). Furthermore, we down-sampled each RGB image to 3x50x75 pixels to reduce computation time. Trial and errors showed that higher resolutions or image preprocessing enhancements such as CLAHE do not necessarily improve the results.

4. Neural Network Method results

The following three neural networks were found to be the best:

ANN 1: first hidden layer with 400 nodes, and second hidden layer with 10 nodes, resulting in best-run correlation coefficient of 0.6578 (ANN vascularity estimate vs. HVS, over validation dataset). This correlation coefficient over the whole dataset (training and validation) is 0.7850.

ANN 2: first hidden layer with 900 nodes, and second hidden layer with 10 nodes, resulting in best-run correlation coefficient of 0.6365 (ANN vascularity estimate vs. HVS, validation dataset). This correlation coefficient over the whole dataset (training and validation) is 0.8170.

ANN 3: first hidden layer with 800 nodes, and second hidden layer with 30 nodes, resulting in best-run correlation coefficient of 0.5959 (ANN vascularity estimate vs. HVS, validation dataset). This correlation coefficient over the whole dataset (training and validation) is 0.8723.

To further enhance ANN results, we used a simple sum (average) rule to create a committee of the above three networks, as it is known that given the independence of the output errors, such committee can improve the estimation results [14]. Eventually, the correlation coefficient for the ANN committee' s output vs. HVS target was 0.8865 (calculated over the whole dataset, training and validation). In either case, the ANN method outperforms the heuristic method.

Computational complexity: using the aforesaid committee of trained ANNs (the most complex mode running three neural nets), the average CPU time over 10 different runs was about 0.0497 seconds (computational environment: MATLAB 2012a running on a quad-core 2.8 GHz Intel Core i7 based PC with 8GB of RAM). Under the same conditions, the average computational time for heuristic method was 0.1228 seconds, which is more than twice slower.

III. Conclusion

Given the importance of fast and objective assessment of conjunctival vascularity, here we introduced two methods for estimating conjunctival vascularity from simple RGB captures. The first (heuristic) method provides a rather reasonable result (a correlation coefficient of almost 0.6) when compared to human observer' s assessments, and is simple and relatively fast, but it may fail to correctly evaluate some cases. For instance, prominent vascular patterns with fewer (but thicker) veins tended to be given lower scores.

The neural network-based method is more accurate but at the same time computationally more expensive during training (but not post training). In either case, fusion methods combining different vascularity sub-scores showed promise in improving the overall estimates.

IV. Acknowledgment

We are thankful for the help provided by Vikas Gottemukkula, Pavan Tankasala, and Goutam Nalamati for processing the study data.

References

[1] Kanski J.J., Clinical Ophthalmology, Fifth Edition. Butterworth Heinemann, Oxford, 2003.

[2] Dumbleton KA, Chalmers RL, Richter DB and Fonn D, "Vascular Response to Extended Wear of Hydrogel Lenses with High and Low Oxygen Permeability", Optometry and Vision Science, March 2001 vol. 78, no. 3, pp. 147–151

[3] Santodomingo-Rubido J., Wolffsohn J.S. & Gilmartin B., "Changes in Ocular Physiology, Tear Film Characteristics, and Symptomatology With 18 Months Silicone Hydrogel Contact Lens Wear", Optometry & Vision Science, February 2006 - Volume 83 - Issue 2 - pp 73-81.

[4] P.A Gardiner, "Observations on the transparency of the Conjunctiva*", British Journal of Ophthalmology Nov 1944 pp. 538-54

[5] Heath G., "The episclera, sclera and conjunctiva. An overview of relevant ocular anatomy", Differential Diagnosis of Ocular Disease, Module 9, Part 2

[6] IER Grading Scales. Institute for Eye Research, Sydney, Australia. Available at: http://www.siliconehydrogels.org/grading_scales/SETUP.HTM.

[7] Efron N., "Clinical application of grading scales for contact lens complications", Optician. 1997; 213 (5604): pp. 26 –35

[8] Duench S., Simpson T., Jones L.W., Flanagan J.G., Fonn D., "Assessment of variation in bulbar conjunctival redness, temperature, and blood flow" Optometry & Vision Science. 2007 June; 84(6): pp. 511–516

[9] Schulze M, Hutchings N, Simpson T., "The use of fractal analysis and photometry to estimate the accuracy of bulbar redness grading scales" Invest Ophthalmology Vision Science. 2008; 49: pp. 1398–1406.

[10] J. Daugman, "How iris recognition works," *Circuits and Systems for Video Technology, IEEE Transactions on,* vol. 14, pp. 21-30, 2004.

[11] R. Derakhshani and A. Ross, "A Texture-Based Neural Network Classifier for Biometric Identification using Ocular Surface Vasculature," in *Neural Networks, 2007. IJCNN 2007. International Joint Conference on*, 2007, pp. 2982-2987.

[12] R. C. Gonzalez, R. E. Woods, and S. L. Eddins, *Digital Image processing using MATLAB*: Dorling Kindersley, 2004.

[13] S. S. Haykin, *Neural networks and learning machines*, 3rd ed. New York: Prentice Hall, 2009.

[14] C. M. Bishop, *Pattern recognition and machine learning*. New York: Springer, 2006.